

# Dynamic properties of the lamprey's neuronal circuits as it drives a two-wheeled robot

**Amir Karniel**

Department of Electrical Engineering, Technion – Israel Institute of Technology, Haifa, Israel  
karniel@ee.technion.ac.il

**Karen M. Fleming**

Department of Physiology, Northwestern University Medical School, Chicago, Illinois, USA  
kflaming@northwestern.edu

**Vittorio Sanguineti**

Departmento di Informatica Sistemistica E Telematica, Università di Genova, Genova, Italy  
sanguini@dist.unige.it

**Simon Alford**

Biological Sciences, University of Illinois at Chicago, Chicago, Illinois, USA  
sta@uic.edu

**Ferdinando A. Mussa-Ivaldi**

Department of Physiology, Northwestern University Medical School, Chicago, Illinois, USA  
sandro@northwestern.edu

## Abstract

In order to study the neurobiological mechanisms of learning, we developed a research tool that includes the brainstem of a lamprey and a two-wheeled robot interconnected in a closed loop. Two electrodes applied stimulations to the neural tissue. The stimulation frequency was set to be proportional to the light intensity measured by sensors on the right and left sides of the mobile robot. The velocity commands to the right and left wheels were proportional to the population spike rates recorded by two recording electrodes. In most cases, the robot moved approximately in the direction of the source of light.

We fitted ten two-input/two-output neural network models and observed the generalization error of each model. We found that a dynamic model was significantly superior to a static model even when the number of parameters was smaller. Additional findings led us to conclude that the main origin of this dynamic behavior is local ipsilateral influence of the previous state on the current state. An analysis of the model that fits adaptive behavior of the preparation showed a significant change in one of the recurrent connections. We discuss these results in the context of possible cellular mechanisms that might explain the behavior of this neuro-robotic preparation.

## 1. Introduction

Interconnecting artificial systems to the human body is an old engineering dream with promising applications for the physically disabled and for extending the functionality of the old as well as the young (see Levine et al. 2002). The crown of this research is the attempt to interconnect and augment the human brain. Recent studies in monkeys showed that the information measured in the motor cortex could be used to guide a robotic arm or to move a computer cursor. (Wessberg et al. 2000, Mussa-Ivaldi 2000, Serruya et al. 2002). However, teaching a monkey (that sees the robotic arm) to control it is still a daunting task (Helms Tillery et al. 2001, Taylor and Schwartz 2001). In order to study adaptation in a simple biological motor control system, we have developed a research tool that includes a portion of living brain tissue of a lamprey and a two-wheeled robot interconnected in a closed loop (Reger et al. 2000).

The Lamprey is an eel-like fish, whose nervous system has been extensively studied particularly for what concerns its ability to generate and modulate locomotor behavior (Grillner et al. 2000). We have selected a portion of the neural circuitry that in normal circumstances receives vestibular and other sensory signals and issues motor commands to stabilize the orientation of the body during swimming (Rovainen 1979, Deliagina 1997). This system has been shown to be adaptive, as unilateral lesions

of the vestibular capsules are followed by a slow reconfiguration of neuronal activities until the correct postural control is recovered (Deliagina 1997).

In our hybrid system, vestibular signals were replaced by light intensity signals. Two electrodes applied stimulations to the axons of the octavomotor nuclei. The stimulations rates were proportional to the light intensity measured by sensors on the right and left sides of the mobile robot. The mobile robot has two wheels that received velocity commands proportional to the population spike rates recorded by two electrodes in the spinal cord. Therefore, the natural stabilizing behavior – in which the lamprey tracks the vertical axis – corresponds, in the hybrid system to tracking a source of light. Indeed in most cases the robot moved towards the source of light.

The nervous system between the four electrodes assumed the function of a controller, with two inputs and two outputs that determine the behavior of the robot in a closed feedback loop. In this paper we concentrate on the analysis of various possible neuronal models for this controller. Section 2 describes the hybrid system, i.e., the neuronal preparation, the robot and the interface (see also Reger et al. 2000). Section 3 describes the experimental protocol, and section 4 describes the data analysis and the various models that were considered. Then the results are presented in section 5 and discussed in section 6.

## 2. The hybrid system

The system includes three elements: neuronal preparation, a robot and an interface (Figure 1).

### 2.1 The neuronal preparation

The neural component of the hybrid system is a portion of the brainstem of the Sea Lamprey (*Petromyzon marinus*) in its larval state. After anesthetizing the larvae with tricane methanesulphonate, the whole brain was dissected and maintained in continuously superfused, oxygenated and refrigerated Ringer's solution; details in Alford et al. (1995).

We recorded extracellularly the activity of neurons in a region of the reticular formation, a relay that connects different sensory systems (visual, vestibular, tactile) and central commands to the motor centers of the spinal cord. We placed two recording electrodes in the axons of the right and left Posterior Rhombencephalic Reticular Nuclei (PRRN). We also placed two unipolar tungsten stimulation electrodes among the axons of the Intermediate and Posterior Octavomotor nuclei (nOMI and nOMP). These nuclei receive inputs from the vestibular capsule and their axons form synapses with the rhombencephalic neurons on both sides of the midline. The recorded signals were acquired at 10kHz by a data acquisition board (National Instruments PCI-MIO-16E4) on a Pentium II 200MHz computer (Dell Computer Corp.).

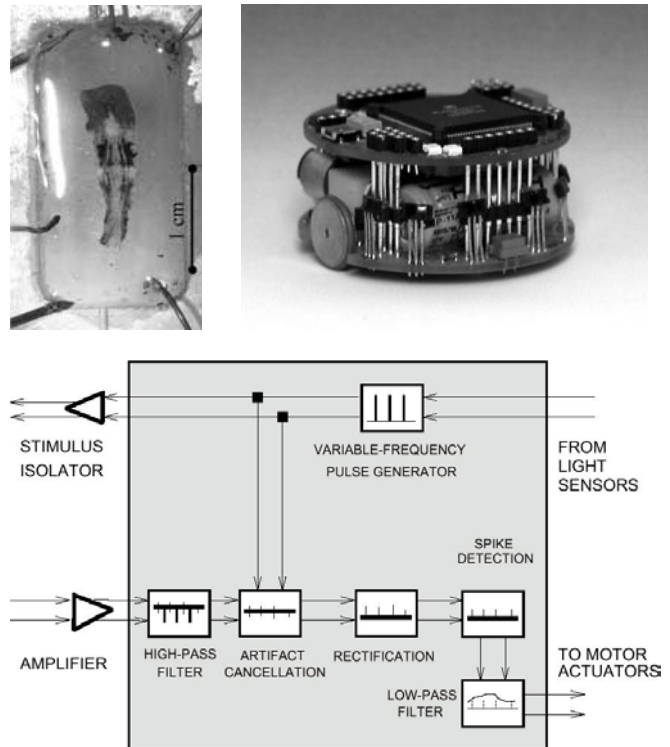


Figure 1: The Hybrid system: The neuronal preparation, a lamprey's brainstem in a physiological solution (Top-left). The two-wheeled robot (Khepera module, Top-right). The interface (Bottom) between the robot (right) and the Lamprey preparation (left) implemented in LabVIEW.

While the axons of the nOMI remain ipsilateral, those of the nOMP cross the midline. As a result, the activity of one vestibular capsule affects both the ipsi- and contralateral reticulospinal (RS) nuclei. We placed each stimulating electrode near the region in which the axons of the nOMI and nOMP cross. This placement of the electrodes also induced predominantly excitatory responses in the downstream neurons. The recording electrodes were placed on either side of the midline, near the visually identified neurons of the PRRN. To verify the placement of the stimulating electrodes we delivered brief single stimulus pulses (200 $\mu$ s) and observed the response in both the ipsi- and contralateral PRRN neurons. Once it was determined that the stimulation electrodes were properly placed, the recording electrodes were moved caudally in order to pick up population spikes. In some experiments, the stimulation had a biphasic (negative current followed by a positive current) rather than a monophasic (negative current only) waveform. The biphasic stimulation was used because it causes less charge buildup and less redox reaction at the stimulating electrode surface. This has the effect of increasing the length of time the preparation is stable and decreasing the likelihood of tissue damage during the barrage of stimuli that accompanies "sensing" and moving in the robot.

## 2.2 *The robot and the workspace*

The robot system is the base Khepera module (K-Team; Figure 1). Its small size allowed us to use a small workspace (Figure 2). A circular wall was constructed with a 2 foot diameter and then painted black to reduce the amount of reflected light. Placed along the circumference of the robot are eight sensors each providing proximity and light intensity information. The sensors are located on opposite sides of the robot's midline at 10°, 45°, 85°, and 165° from the front position. Two wheels provide a means of locomotion for the small robot. Our computer system communicates with the robot through the serial port and a custom designed LabVIEW© application. Eight lights are mounted at the edge of the robot workspace at 45° intervals. The lights are computer controlled using the digital outputs of our acquisition card. These lights generate the stimulus that elicits a phototactic response.

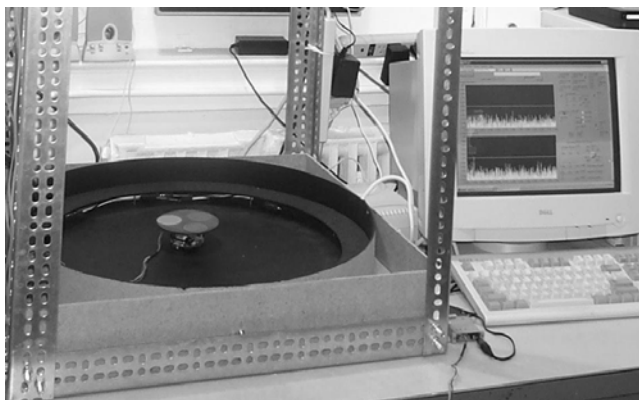


Figure 2: The robot in the workspace and typical screen of the LabView program that implement the interface to the neuronal tissue of the Lamprey.

## 2.3 *The interface*

The interface acts as an interpreter between the neural signals and the robot control system (Figure 1). It is responsible for the transformation of the robot's light sensor information into vestibular inputs and then processing in real time the neural activity of the reticulospinal nuclei and translating it into motor commands for the robot.

The light intensities detected by the robot sensors determine the frequencies at which the right and left vestibular pathways are stimulated. As stated above, there are eight light sensors on the robot. We weight the sensors to give the greatest strength to sources of light that come at 45° and to ignore the rear sensors. The weighted sum of the sensors on each side is multiplied by a gain factor, which determines the maximum stimulation frequency. The final result is the frequency at which we stimulate each side. We use the digital counter on the acquisition board to generate a pulse train. This pulse train is delivered to the neural preparation by the tungsten electrodes after passing through ISO-Flex stimulus isolators.

The spiking activities of the PRRN as recorded near the axons are analyzed through a five steps process (Figure 1). The signal picked up by the recording electrodes contains a combination of spikes, stimulus artifacts, excitatory and inhibitory postsynaptic potentials (PSP) and noise. To suppress the slow PSP components, this signal is first put through a high pass filter (cutoff at 200 Hz). The output of this filter contains high frequency noise, stimulus artifacts, and the spikes generated by multiple neurons in the vicinity of the electrode. Stimulus artifacts are canceled by zeroing the recorded signals over temporal windows of 4 ms following the delivery of each 200  $\mu$ s triggering pulse. The remaining signal is rectified, and a threshold is applied to separate the spikes from the background noise - under the assumption that the spike amplitude is much larger than the noise amplitude. The resulting train of spikes is put through a low pass filter (5 Hz), which effectively generates a rate coded signal. The mean of this signal over 300 milliseconds is used as a velocity control signal for each of the robot's wheels.

## 3. **Experimental protocol**

### 3.1 *Interface calibration*

The interface was calibrated so as to account for random differences between the recorded responses from the left and right side of the brainstem. Indeed, the net intensity of the signal picked up by each electrode is affected by a number of uncontrollable factors, such as the actual distance from signal sources. To compensate for these random factors, we made the working assumption that when both left and right sides are stimulated at the same frequency, the same motor response should be obtained on each side of the robot. This corresponds to considering all initial asymmetries between right and left side as accidental features of no significance. Accordingly, all initial difference between right and left responses to the same right and left signals were balanced by regulating two output gains.

In most cases, the right and left sides of the neural preparation were connected both in input and in output with the corresponding sides of the robot (direct mode). However, in some cases it was necessary to implement a reverse mode option. When connected in reverse mode, the right recording electrode is connected through the interface to the controller of the left wheel and vice versa.

### 3.2 *Plasticity Protocol*

Following studies that demonstrated compensation in behaving lampreys (Deliagina 1997), we tested the hypothesis that we could induce a plastic change in neural connections using the following protocol: First, we electronically "blinded" the left side of the robot by substantially reducing the gain of the light sensors on the

left side of the robot from 1.0 to 0.1. Thus, all stimulation to the left side of the lamprey PRRN was eliminated, simulating a unilateral labyrinthectomy or lesion in the lamprey. Next, the robot moved about the workspace for 20 min, guided by random stimulation provided by either following a flashlight held by the experimenter or moving toward the workspace perimeter lights after starting from the center of the workspace. Trajectory sets were measured (with the gain of the left light sensors at 1.0) for an hour before the plasticity protocol and for an hour afterwards allowing a resting period of 5-10 minutes between trajectory sets.

#### 4. Neuronal Models

The purpose of the hybrid system is to investigate the computational properties of neural tissue. For each individual experiment, we obtained a model of the empirical input/output transformation for the left and right PRRN by fitting a bivariate function to the light sensor data (stimulus/input) and wheel motor commands (response/output). In this section we describe the various models that were considered and the data for the fitting and testing procedure.

##### 4.1 Ten models

Each model is a two inputs two outputs system. Let  $u_L$  and  $u_R$  indicate light intensity transformed into the frequencies of the stimuli delivered by the left and right electrodes and let  $y_L$  and  $y_R$  indicate the firing rates

recorded in response to these stimuli from the right and left PRRNs transformed into wheel speeds directed to the robot's wheels. Then, a simple model for the lamprey's brain is the following static linear model (see Figure 3a).

$$y_L(n) = w_{LL}u_L(n-1) + w_{LR}u_R(n-1)$$

$$y_R(n) = w_{RL}u_L(n-1) + w_{RR}u_R(n-1)$$

The parameters,  $w_{ij}$ , were determined by least-square approximation of the input/output data and form collectively a  $2 \times 2$  matrix  $W$ . The elements of  $W$  can be considered as *connection weights* between vestibular axons and reticular neurons. Positive weights represent excitatory connections and negative weights inhibitory connections. This simple linear static model (Figure 3a) can generate various behaviors, such as moving towards a light, away from the light or circling a light source (see Braitenberg 1984). We used this model as a baseline and compared the performance of other more complex models to this linear static model. For each lamprey and in each condition during the experiment, the data of one set of trajectories (testing set) were not used for the fitting. The parameters that best approximated the rest of the data (fitting set) were used to predict the network output over this testing set of trajectories. This procedure was repeated for each set of trajectories in order to achieve a good estimate of both fitting and testing (i.e., generalization) errors.

We also considered nonlinear functions of the inputs,

$$y_L(n) = P_L\{u_L(n-1), u_R(n-1)\}$$

$$y_R(n) = P_R\{u_L(n-1), u_R(n-1)\}$$

where  $P_{L,R}$  are polynomial functions (polynomial

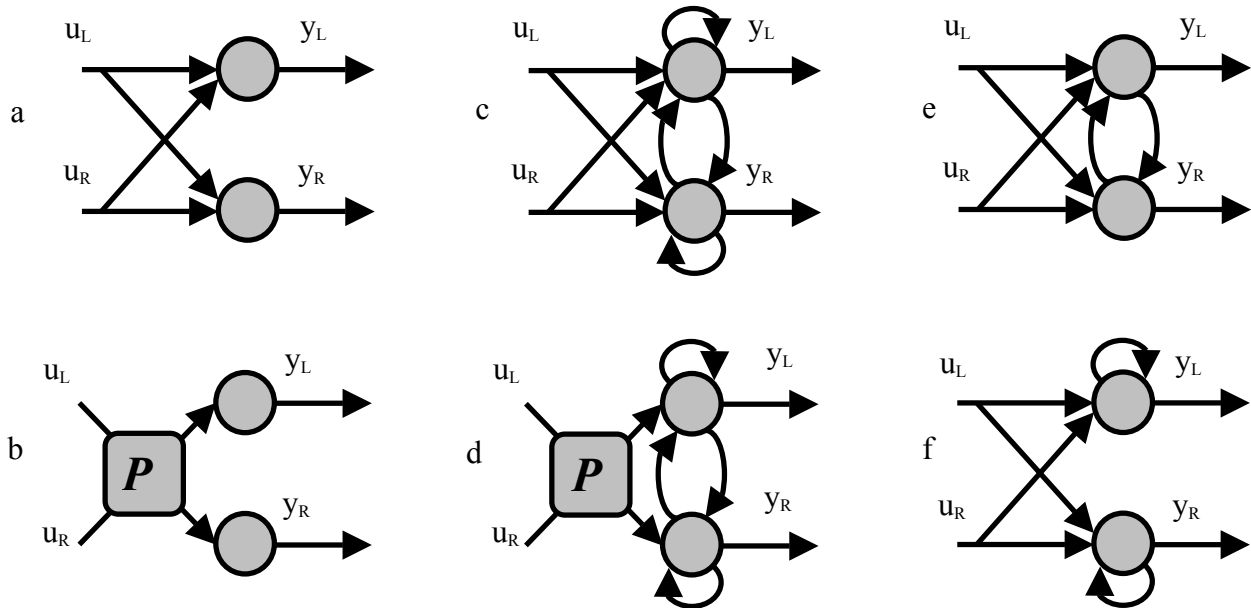


Figure 3: Models for the Lamprey's brainstem circuits between the electrodes. a. Static linear model. b. Static polynomial model. c. Dynamic linear model. d. Dynamic model with polynomial input function. e. Dynamic linear model without ipsilateral dynamic connections. f. Dynamic linear model without contralateral dynamic connections.

functions are known to be capable of approximating any smooth function). For example a second order polynomial model took the following form:

$$\begin{aligned}
 y_L(n) &= a_{L1}u_L(n-1) + a_{L2}u_R(n-1) + a_{L3}u_L^2(n-1) + \\
 &+ a_{L4}u_R^2(n-1) + a_{L5}u_L(n-1)u_R(n-1) \\
 y_R(n) &= a_{R1}u_L(n-1) + a_{R2}u_R(n-1) + a_{R3}u_L^2(n-1) + \\
 &+ a_{R4}u_R^2(n-1) + a_{R5}u_L(n-1)u_R(n-1)
 \end{aligned}$$

In this study, we considered polynomials up to the 4th degrees. The number of parameters increased with polynomial degrees as follows: 2nd degree, 10 parameters; 3rd degree, 18 parameters; 4th degree, 28 parameters.

Furthermore, we explored the additional explanatory power of linear dynamic models, i.e., models that take into account the previous neuronal activity and therefore represents recurrent loops and/or memory phenomenon in the time scale of seconds. The first order dynamic model was the following (see Figure 3c)

$$\begin{aligned}
 y_L(n) &= w_{LL}u_L(n-1) + w_{LR}u_R(n-1) + \\
 &+ v_{LL}y_L(n-1) + v_{LR}y_R(n-1) \\
 y_R(n) &= w_{RL}u_L(n-1) + w_{RR}u_R(n-1) + \\
 &+ v_{RL}y_L(n-1) + v_{RR}y_R(n-1)
 \end{aligned}$$

We then considered polynomial input functions as described above with the dynamic model, and finally, since the first order static model was found to be most appropriate, we also explored the role of ipsilateral and contralateral connections by considering two models that included only one type of these connections (see Figure 3e,f). Altogether we have considered four static models, and six dynamic models.

## 4.2 The data for fitting and testing

The basic set of data is a single trajectory of the robot that starts to move from the center of the workspace (Figure 2), as a response to a light that is turned on. We used the values of inputs and outputs measured and generated at the time steps of the control loop (twice in each second). Each of the five lights was turned on - one after the other - with a short break for returning the robot to the initial position. Each trajectory lasted about 5-10 seconds and typically contained more than 10 sampling points. In each condition (before and after adaptation/control protocol), a few sets of 5 trajectories were recorded (typically 4 sets). To explain the fitting and generalization error calculations in each condition, we denote the number of sets (each of 5 trajectories) by  $n$ . For the  $n$  possible combinations of  $n-1$  sets, each model was best fitted to the data of  $5*(n-1)$  trajectories yielding the least mean square error (MSE). The parameters of the best model were used to predict the output of the other set that was not used for the fitting. The mean over the  $n$  sets of each error (fitting and testing) was calculated and is referred to as learning error and generalization error for

that condition. Then, the mean over preparations and over different conditions was calculated. Note that the bootstrapping method of choosing every possible combination was used to gain an accurate estimation of the actual MSE for the learning and generalization. However, for the statistical tests reported in the results section, the MSE for each condition was used just once. For further details about cross validation and the problem of overfitting, see, e.g., Haykin (1999), Karniel and Inbar (2000).

We report the fitting results over the data gathered from 31 preparations before and after adaptation/control experiment. Therefore, 620 values of learning errors and the same number of generalization errors were the output of this data analysis.

## 4.3 Simulation of the whole system

In order to compare the capabilities of the neuronal models we have conducted simulation of the whole system. These simulations combined a discrete neural model (Figure 3) with a continuous model for the robot and the sensors.

For the continuous model, the state variables were the position and orientation of the robot. The light intensity observed by the sensors at the right and left sides of the robot was calculated according to the geometry of the system. The light intensity at each side was a function of the robot's state and of the location of the light. Since the control signal dictates the velocity of the wheels and since the mass of the robot is negligible, the result was a first order nonlinear system (see Reger et al. 2000 for further details). This first order dynamic system was controlled by the discrete neuronal model. The neural model was either static (Figure 3a,b) or first order dynamic (Figure 3c-f).

## 5. Results

We have analyzed the fitting of various models to the neuronal tissue of the lamprey brainstem as it drives the two-wheeled robot. We found that the dynamic properties are significant and, in particular, the ipsilateral dynamic properties. Here, we report our fitting results for the various models and for a few preparations with transected spinal cord. Then, we demonstrate the plasticity in one example, and report the analysis of the change in weights of the best model for nine preparations that displayed clear plasticity. Altogether, our analysis indicates that the dynamic model with ipsilateral connections (Figure 3f) is the best model among the 10 tested models and that the dynamic properties are essential in order to account for behavior as well as for plasticity.

### 5.1 Dynamic properties

In our endeavor to understand the synaptic pathways involved in the observed behaviors, we modeled

the connections with polynomials of increasing order, and with static as well as dynamic models (see Figure 3 and the Methods section). Figure 4 shows these results.

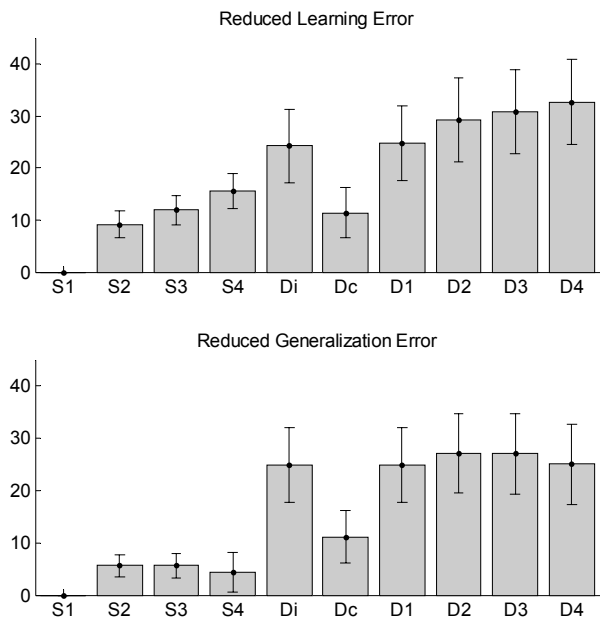


Figure 4: The reduced fitting (learning, upper plot) and testing (generalization, lower plot) errors with various neuronal models measured in percents. The baseline is a linear static model (S1), and the rest of the bars stands for polynomial models upto fourth order (S2-4), dynamic linear model (D1) and dynamic model with polynomial input function upto fourth order (D2-4). Di stands for dynamic linear model without contralateral connections, and Dc stands for dynamic linear model without ipsilateral connections.

The data clearly indicate a greater error reduction with the dynamic scenarios over the static, even when the static models include more parameters. The upper bar plot in Figure 4 shows learning errors. It is obviously expected that the error would be smaller with the increase in the complexity of the model. The lower bar plot shows the generalization error, which is the error over data that were not used for the fitting. Note that the advantage of the dynamic model appears both in the fitting and in the testing errors. A one-way analysis of variance (ANOVA) over the generalization errors of the eight models (S1-4, and D1-4) clearly rejects a null hypothesis that the models' mean errors are equal ( $p < 0.01$ ). A Student's t-test shows that the mean error of the first order dynamic model is significantly lower than the errors of a first and a second order static model ( $p < 0.01$ ). The first order dynamic model reduced the error by 25%. In contrast, adding further complexity to the model led only to reduce the error by a few percentage points. Therefore, the first order dynamic model (Figure 3c) was selected for further analysis as a better candidate than any static model. One should remember that this is an average over preparations and over trajectories to different light sources. As this average included many data points, it hides many details. Nevertheless, the advantage of

dynamic model, which contains just 8 parameters, over any static model is apparent.

## 5.2 Two types of recurrent connections

The anatomy of the Lamprey's nervous system does not support the presence of direct connections between reticular neurons on the two sides of the midline. Therefore it would be difficult to explain the contralateral connections in our model. Accordingly, we have considered separately a model without recurrent contralateral connections (Figure 3f), and a model without recurrent ipsilateral connections (Figure 3e). The analysis clearly supports our expectations (see the two middle bars in Figure 4). Guided by Occam's razor principle among the equally good models, we favor the model with the fewer parameters, which is the dynamic linear model with only recurrent ipsilateral connections (Figure 3f). Note that this linear model with just six parameters outperformed all the static linear and nonlinear models.

The known anatomy suggests the presence of pathways from the brainstem to the spinal cord and back (see e.g., Grillner et al. 2000). This is one possible explanation for the improved fitting of models with dynamic connections. In order to test this hypothesis we have transected the spinal cord in four preparations and repeated the same protocol. These preparations generated similar results as generated with intact spinal cord. The learning and generalization were similar to Figure 4, and in particular, the reduced error with dynamic model was still about 25%. Therefore we conclude that the recurrence afforded by bi-directional spinal cord pathways is not the likely reason for the dynamics expressed by the recurrent connections in the model. In the discussion section we describe alternative accounts for the observed dynamic properties.

## 5.4 Dynamic properties and behavior

In order to demonstrate the implications of the neuronal model on the possible behavior of the robot, we have simulated the robot movement when it was controlled by the static and the dynamic neural models (Figure 5).

In this example, the static model was a first order model (Figure 3a) with weights values of 0.5 at the crossing connections. The dynamic model was first order (same values of weights) with only ipsilateral connections, again with a value of 0.5 (Figure 3f).

While all the tested models are capable of generating a broad repertoire of behaviors in response to the presentation of sources of light, there are some subtle but potentially important differences in the robot trajectories produced by static and dynamic models. For example (Figure 5), models with recurrent dynamics tend to display more undulations in the trajectories than strictly static models. This seems to reflect the presence of second order dynamics in the neuro-robotic system.

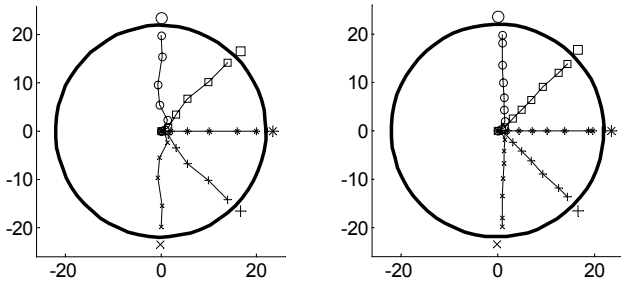


Figure 5: Simulation of the robot behavior. Each symbol represents the location of a light source and the trajectory of the robot when that light was turned on (in the simulation). The controller was either a static linear model (right) or a dynamic first order model with only ipsilateral connections (left).

### 5.5 Weights' change during adaptation

Figure 6 shows a typical result of the plasticity protocol, indicating a tendency of the robot to turn to the right after a period of training with the left sensor occluded. Both sets of trajectories were obtained in identical conditions, with inputs from both right and left sensors.

The change in direction can be accounted for both by a reduction in the spinning of the right wheel and by an increase in the spinning of the left wheel. Therefore both a

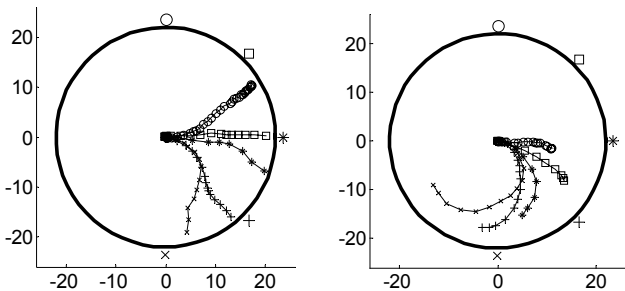


Figure 6: Five trajectories of the robot before (left) and after (right) the plasticity protocol. Each symbol represents the location of each light source and the trajectory of the robot when that light was turned on. Both sets of trajectories were obtained in identical conditions, with inputs from both right and left

potentiation of the synapses on the left or a depression of the synapse on the right or a combination of both could lead to the observed behavior.

To establish which kind of synaptic change was actually responsible for the change in robot's motion, we selected the preparations that resulted in a significant adaptive rotation to the right ( $n=9$ ) and fitted the first order dynamic model with recurrent ipsilateral connections (Figure 3f, 6 parameters). The values of these parameters before and after the plasticity protocol were compared and the difference is presented in Figure 7. The reduction in the recurrent ipsilateral connection of the right side is consistent with the turn to the right. It is interesting that the most significant change occurred in the dynamic connection and we are currently interpreting it as a general

reduction in the responsiveness of the reticular neurons on the right side, induced by a period of reduced contralateral input from the left vestibular afferents.

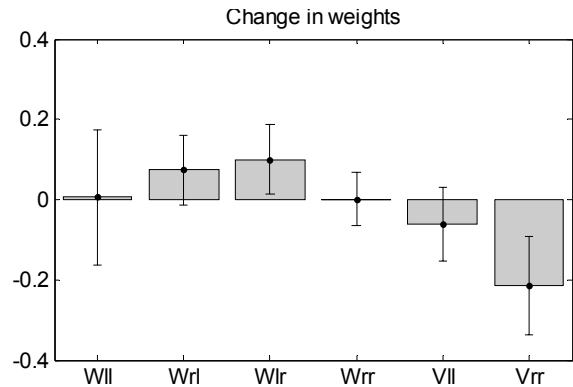


Figure 7: Change in the weights of the dynamic linear model without crossing connections (Figure 3f) before and after the plasticity protocol.

## 6. Discussion

We used a hybrid neuro-robotic system to study the properties of the neural tissue in the brainstem of a lamprey as it drives a two-wheeled robot. We have found that the best model of this tissue is a dynamic linear network with recurrent ipsilateral dynamic connections.

### 6.1 The dynamic properties

The introduction of recurrent ipsilateral connections appeared indeed to be essential for improving the ability of our network models to capture the dynamical behavior of the hybrid system. We discuss here two possible reasons for this result.

One possibility is that the recurrent dynamics are due to an actual neuronal pathway. We considered the possibility for contralateral pathways and for pathways to the spinal cord and back. But we found that a surgical transection of the spinal cord does not abolish the observed dynamical behavior. Therefore, a neuronal pathway to account for this result should be spatially limited to a local region in the proximity of the PRRN. However, this seems to be at odds with the fact that the delays involved in our simulations are of the order of hundreds of milliseconds.

Another, more likely, interpretation suggest the presence of a local memory mechanism within each neuron (see Kandel et al. 2000 to explore the various possibilities). This could be any mechanism, such as the threshold for plateau potential, capable of establishing a relation between the tendency of a neuron to fire at one instant of time with the state of the neuron a few hundred milliseconds before. What matters here is for the neurons activity not to depend exclusively upon the instantaneous synaptic input.

It is important to mention that we have specifically chosen to place our electrodes far from neurons

that are firing spontaneously. The electrode placement was chosen such that there would be no firing without any input stimulation. Nevertheless, it is possible that some sort of protracted firing was generated by these neurons or was induced by other nearby neurons.

## 6.2 The neuro-robotic system

Hybrid neuro-robotic systems provide an artificial environment that is amenable to precise control by the experimenter for studying the operation of the nervous system. In this investigation we have introduced a “reversible artificial lesion” by changing the output gain of light sensors. We see this procedure as alternative to irreversible surgical manipulations, such as the removal of a vestibular organ (unilateral labyrinthectomy). One clear advantage of the artificial lesion over the actual lesion is the possibility to undo the lesion electronically (e.g., “unblinding”). Another case for such neuro-robotic interfaces was recently presented by Zelenin et al. (2000). In their study an electrical motor was used to rotate the lamprey and therefore provide feedback through the natural sensory system of the lamprey rather than through direct excitation, as in our study.

A significant feature of neuro-robotic interfaces is the control that is offered to the experimenter over the exact feedback that is provided through the mechanical system and its sensors. By manipulating this feedback it is possible to study neural mechanisms, such as the dependence of plastic changes upon the correlation between presynaptic input and postsynaptic activity.

Investigation of the rules that govern synaptic plasticity in a hybrid system may lead to finding some effective methods for “programming” neural tissue so that it can execute a desired task. This goal is of central importance for the development of effective neural prostheses. Indeed, once a signal interaction is established between brain tissue and an external device, one can expect that the properties of the neurons interacting with the device will evolve based on the history of signal exchange. Neural plasticity is perhaps the most important resource for establishing a working interaction between brain and external devices. Neuro-robotic interfaces provide a new instrument for the direct investigation of how plasticity can be harnessed for generating a desired behavior.

## Acknowledgments

This work has been sponsored by ONR grant #N00014-99-1-0881.

## References

Alford S., Zompa I., Dubuc R. (1995) Long-term potentiation of glutamatergic pathways in the lamprey brainstem. *Journal of Neuroscience*, 15:7528-7538

- Braitenberg V. (1984) *Vehicles – experiments in synthetic psychology*. MIT press, Cambridge, MA.
- Deliagina T.G. (1997) Vestibular compensation in lampreys: Impairment and recovery of equilibrium control during locomotion. *Journal of Experimental Biology* 200:1459-1471
- Grillner S., Cangiano L., Hu G.-Y., Thompson R., Hill R., Wallén P. (2000) The intrinsic function of a motor system – from ion channels to networks and behavior. *Brain Research* 886:224-236
- Haykin S. (1999) *Neural Networks: A Comprehensive Foundation* 2<sup>nd</sup> edition, Prentice Hall.
- Helms Tillery S.I., Lin W.S.; Schwartz A.B. (2001) Training non-human primates to use a neuroprosthetic device. *Society for Neurosciences Abstracts*:63.4.
- Kandel E.R., Schwartz J.H., and Jessell T.M. (Eds.) (2000) *Principles of neural science*. 4<sup>th</sup> edition, McGraw-Hill
- Karniel A., Inbar G.F. (2000) Human Motor Control: Learning to Control a Time-Varying Non-linear Many-to-One System. *IEEE transactions on Systems, Man, and Cybernetics Part C* 30:1-11
- Levine M., Roberts L., Smith O. (Eds.) (2002). *Bodybuilding: The Bionic Human - special section*. *Science* 295:995-1033
- Mussa-Ivaldi S., (2000) Neural engineering: Real brains for real robots. *Nature* 408:305-306
- Reger B., Fleming K.M., Sanguineti V., Alford S., Mussa-Ivaldi F.A. (2000). Connecting Brains to Robots: An Artificial Body for Studying the Computational Properties of Neural Tissues. *Artificial Life* 6: 307-324
- Rovainen C.M. (1979) Electrophysiology of vestibulospinal and vestibuloreticulospinal systems in lampreys. *Journal of Neurophysiology* 42:745-166
- Serruya M.D., Hatsopoulos N.G., Paninski L, Fellows M.R., and Donoghue J.P. (2002) Brain-machine interface: Instant neural control of a movement signal. *Nature* 416:141 - 142
- Taylor D.M., Schwartz A.B. (2001). Direct 3D control of an upper limb neural prosthesis using motor cortex cells trained in a brain-controlled virtual movement task. *Society for Neurosciences Abstracts*:129.6
- Wessberg J., Stambaugh C.R., Kralik J.D., Beck P.D., Laubach M., Chapin J.K., Kim J., Biggs S.J., Srinivasan M.A., Nicolelis M.A.L (2000) Real-time prediction of hand trajectory by ensembles of cortical neurons in primates *Nature* 408:361-365
- Zelenin P.V., Deliagina T.G., Grillner S., Orlovsky G.N. (2000) Postural control in the lamprey: a study with a neuro-mechanical model. *Journal of Neurophysiology* 84:2880-2887